doi: 10.32131/jes.2.55

Journal of the Earth Simulator, Volume 2, March 2005, 55–69

A simulation study of the 2003 heatwave in Europe

Mototaka Nakamura*[1], Takeshi Enomoto[2] and Shozo Yamane[1]

[1] *Frontier Research Center for Global Change, Japan Agency for Marine-Earth Science and Technology, Yokohama, Japan*

[2] *The Earth Simulator Center, Japan Agency for Marine-Earth Science and Technology, Yokohama, Japan*

(Received November 8, 2004; Revised manuscript accepted January 25, 2005)

Abstract A devastating heatwave that struck much of western Europe during the first two weeks of August, 2003 was studied as a case of strong summer blocking, using high-resolution global atmospheric simulation model output and the NCEP/NCAR reanalyses. From the reanalyses data diagnoses, the heatwave was found to be caused by an eastward shift in the location of a summer blocking that occurs sometimes over the North Atlantic. Further diagnoses reveal a region of anomalously strong vertical flux of high-frequency waves in the central North Atlantic preceding the heatwave, suggesting that it may be a potential cause of the eastward shift. Six simulations of a period, July 1 – August 15 2003, were performed with AFES, using the daily observed SST in the control run and the climatological SST in parts or all of oceans in the other runs. The control run reproduced the heatwave reasonably well, as well as some of the wave forcing found in the reanalyses data. In three other runs that were forced with the climatological SST everywhere or in selected regions did not reproduce the heatwave at all, with a blocking occurring farther west of that in the control run. These runs did not produce the suspected key wave forcing for the heatwave either. The results suggest an important role of the anomalously strong wave forcing in the central North Atlantic in shifting the blocking location and, thus, bringing the heatwave to western Europe.

Keywords: heatwave, Europe, blocking, eddy forcing

1. Introduction

During the first half of August 2003, a large part of western Europe experienced an unprecedented warm condition. The heatwave resulted in loss of thousands of lives in France, not to mention many cases of health problems related to heat exhaustion reported in the region. The estimated daily mean surface temperature (color shade) and its departure from the 30-year (1974–2003) mean (contours) obtained from NCEP/NCAR 6-hourly reanalyses [1] in this region during the heatwave are shown in Fig 1. Note that these are for the average temperature for the day, not for the maximum temperature of the day. Maximum temperatures exceeding 40°C were reported in this region that normally enjoys relatively mild summers with the daily maximum temperature typically ranging from 20°C to 25°C. The anomaly in the daily mean surface temperature in France uring this period is typically 5°C and larger, reaching 11°C in some spots (Fig. 1). In fact, even the daily *minimum* temperature often exceeded the climatological daily *mean* temperature during the heatwave due to accumulation of heat in the soil during the day aided by low soil moisture content [2]. Evidently, the condition for the occurrence of the heatwave was prepared over a few months of warm and dry condition preceding the heatwave.

Schär et al. [3] examined the monthly mean surface temperature in Switzerland and found that an event like the heatwave is highly unlikely to occur in the climate of the past 150 years, and that the anomaly of the mean surface temperature for August 2003 is an offset of some 5 standard deviations from the mean. They further argued that an event like the 2003 heatwave will become more common as a result of increasing variability in a warming scenario produced by a climate change simulation, although credibility of such simulations is highly questionable at best as pointed out in many scientific studies. However, the mechanism for the occurrence of the heatwave that Schär et al. [3] suggested in their study is not inconsistent with the dynamical diagnoses of the heatwave by Black et al. [2] who reported a persistent anticyclonic condition over Europe, accompanied by drying of the land surface over a large area in western Europe during the summer of 2003. The anomalous anticyclonic condition, which is often a sign of blocking, can be seen

* ***Corresponding author***: *Dr. Mototaka Nakamura, Frontier Research Center for Global Change, Japan Agency for Marine-Earth Science and Technology, 3173–25 Showa-Machi, Kanazawa, Yokohama, Kanagawa 236-0001, Japan. E-mail: moto@jamstec.go.jp*

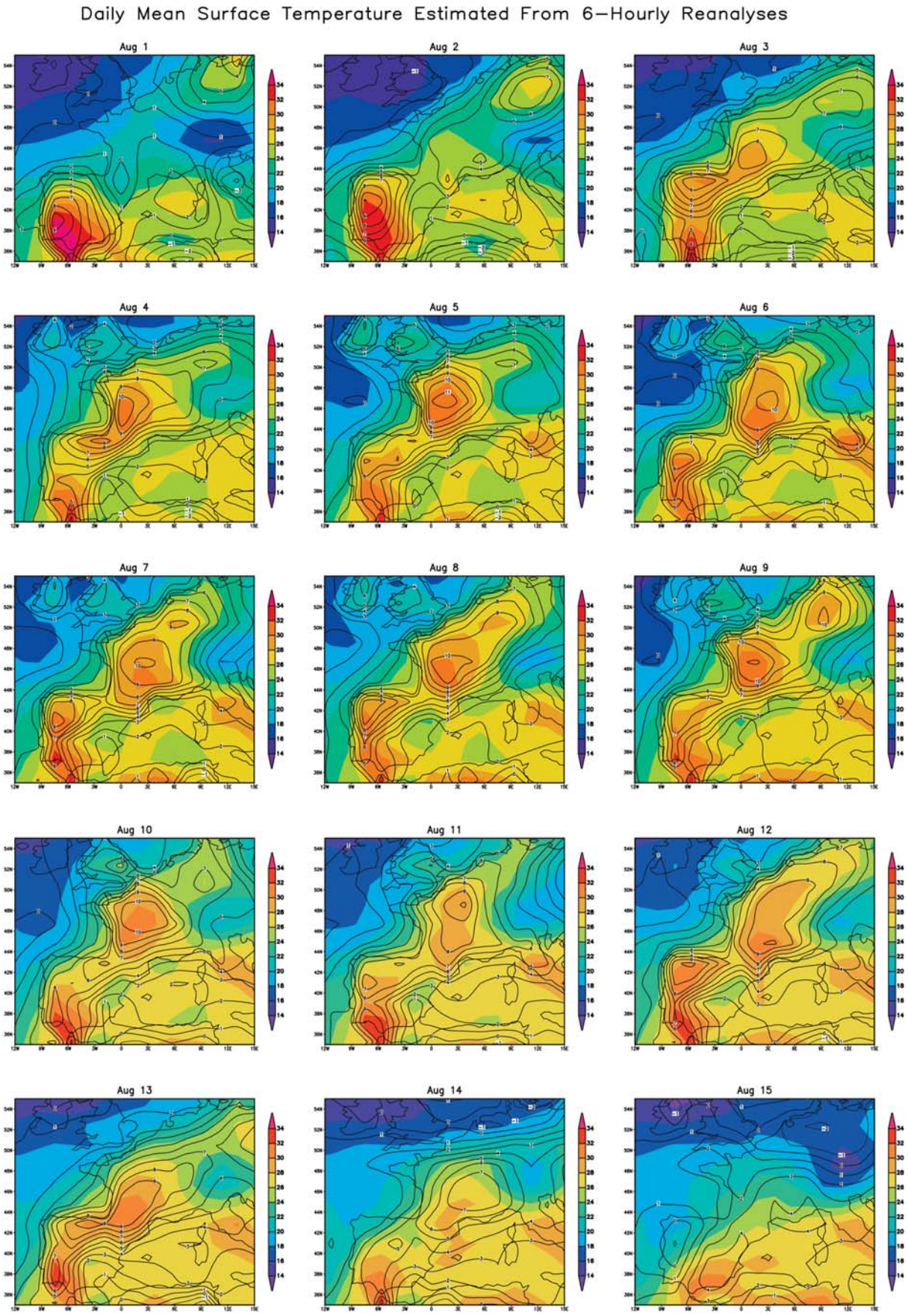

Fig. 1 The daily mean surface temperature (color shade) and its departure (contours) from the 30-year (1974–2003) mean for Aug 1 – 15 during the heatwave in western Europe, estimated from NCEP/NCAR 6-hourly reanlyses.

in the generally positive surface pressure anomaly for August 1 - 15, 2003 in western Europe (Fig. 2). Black et al. [2] reported that the anomalous anticyclonic condition had an equivalent-barotropic structure over Europe, accompanied by an enhanced westerly flow on its poleward flank over UK and southern Scandinavia, suggesting occurrences of a blocking condition there during the 2003 summer. Indeed, as mentioned below, the heatwave was a by-product of a strong summer blocking that brought extremely warm air from northern Africa to western Europe at low levels of the atmosphere.

While the extreme temepratures occurred during the first 2 weeks of August, western Europe was fairly warm from May through August in 2003. Figure 3 shows the departure of the monthly mean surface temperature from a 30-year (1974–2003) climatology for May – August 2003, computed from the NCEP/NCAR reanalyses [1]. As mentioned by Black et al. [2], we find the warm anomaly over western Europe in August having an equivalent-barotropic structure, penetrating up to the lower and middle troposphere. Note that the anomaly in western Europe in August 2003 does not appear particularly abnormal compared with other large temperature anomalies. In fact, the warm anomaly in the central Eurasia in August 2003 appears even more abnormal than that in western Europe. However, a large warm anomaly in a cool area may not be as much a concern as it is in a warm area. Also, a very large anomaly that lasts 2 weeks is likely to be more of a concern than a moderate anomly that lasts 1 month. What contributed to the grave consequenses is the 2 weeks of an extreme condition during the August in a region that is not well-prepared for such extreme warmness. When large-scale dynamical characteristics were examined, the event was found to be a case of strong atmospheric blocking - manifestation of amplification, breaking, and dissipation of a low-frequency planetary-scale wave. It is a nonlinear discretized low-frequency phenomenon [4, 5]. The abnormally high surface temperatures during the event can be attributed to an eastward shift, compared to those typical of the last 30 summers, in the location of the blocking that brought a subtropical air mass of African origin, rather than usual maritime origin, into western Europe. When the effect of a discretized event such as this is viewed as monthly mean anomalies, which is often done in the medium to long range forecasts, the values in August 2003 do not clearly reflect the danger of the heatwave. Because of the nonlinear nature of damages inflicted by a heatwave, and often by other natural disasters (serious losses begin to occur when the condition exceeds a certain threshold), prediction of discretized extreme events such as this is critical to minimize the damages.

Whether prediction of the abovementioned kind is possible is an open question. Although the limit of weather forecasting is believed to be roughly a week or so, it is not certain if the same limit applies to predicting *low-frequency evolution* of the atmosphere associated with planetary-scale waves. These waves have substantially longer time scales than synoptic-scale systems that are often responsible for day-to-day weather changes, and also control behaviors of the synoptic systems to some extent. The major forcing of these planetary-scale waves consists

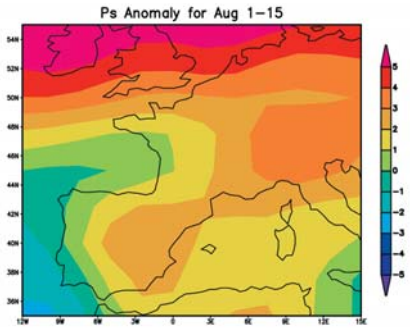

Fig. 2 The departure of the monthly mean surface pressure from a 30-year (1974–2003) climatology, calculated from NCEP/NCAR reanalyses.

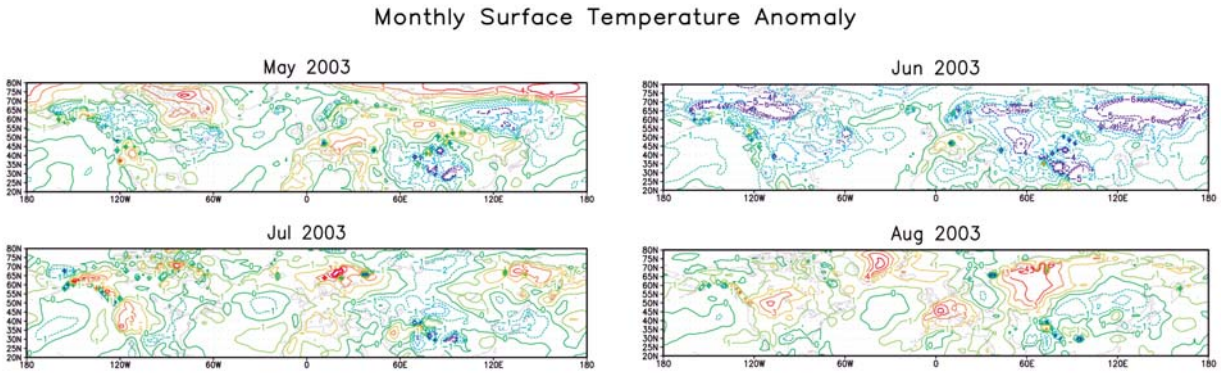

Fig. 3 The departure of the monthly mean surface temperature from a 30-year (1974–2003) climatology, calculated from NCEP/NCAR reanalyses.

of the topography (in combination with the wind over the topography), land-sea temperature contrasts, and ensembles of synoptic-scale waves. Also, these waves have large amplitudes in the stratosphere whose treatment in weather forecasting is far from adequate. An adequate treatment of the stratosphere in weather forecasting is most likely to improve low-frequency evolution of the atmosphere on time scales of tens of days. Thus, the predictability of extreme events that are associated with low-frequency dynamics of the atmosphere seems to be a matter somewhat different from the predictability of the weather, which is controlled by synoptic-scale and mesoscale waves that have time scales of several days and shorter. Perhaps, we may be able to forecast the low-frequency evolution of the atmosphere substantially longer than one week if we can provide an adequate initial condition to a simulation model that represents processes related to the key low-frequency dynamics, including the oceanic fronts. In the advent of super computers that are capable of running a coupled simulation model at an adequately high resolution, such forecasts may become feasible in the future. Needless to say, identifying the key factors that produce low-frequency extreme events and understanding the processes involed in the factors are essential to building a simulation model that is capable of the task.

In this paper, we present a case study of this heatwave, using the output of several experiments performed with AFES, Atmospheric general circulation model For the Earth Simulator [6]. Because of the seemingly low-frequency nature of the dynamics behind the heatwave of 2003, it serves well as a test case for low-frequency state hindcasting. The abnormally cool summer of 2003 in Japan was most likely driven by low-frequency dynamics also, but manifested itself in a mesoscale feature, the "baiu" front, whose dynamics require extremely high spatial resolution. For this reason, the 2003 European heatwave was chosen for this study. However, for reasons discussed below, even the European heatwave requires very high spatial resolution for a successful simulation. We consider a horizontal resolution of 20 km as the coarsest allowed for our study, and that the entire atmosphere needs to be simulated because of the planetary-scale of the waves behind the phenomenon. Running simulation experiments at such spatial resolution is only possible, in a practical term, with the Earth Simulator. We examine the simulated events and briefly compare them with the actual one. We focus on the simulation results here and report detailed study of the heatwave using reanalyses elsewhere. Section 2 describes experiments done with AFES and discusses their results. We offer concluding remarks in section 3.

2. Heatwave simulation by AFES

To investigate potentially important factors behind the heatwave, we performed a series of experiments using AFES, an AGCM designed to exploit the architectures of the Earth Simulator for efficient performance. Due to the limited CPU time and archival space, we focused on two questions: Can we reproduce the heatwave in AFES with the observed daily SST, starting one month before the heatwave? If we can, then, can we identify the regions of SST anomalies (surface temperature gradient anomalies, to be precise) that played important roles in the heatwave?

2.1 Experimental configurations

The resolution used for this study was T639L48, truncation wave number of 639 and 48 vertical levels. There are 6 levels in the planetary boundary layer, 28 levels in the troposphere, and 14 levels in the stratosphere. The choice of high horizontal resolution is based on our belief that diffusive removal of atmospheric filaments and small vortices generated by breaking Rossby waves degrades the quality of medium- to long-term simulation, especially when the target phenomena are highly nonlinear. Also, if strong baroclinic forcings at the oceanic fronts and/or land-sea boundaries play important roles in the target phenomena, a grid size of 50 km or larger cannot adequately resolve the important forcing in the first place. We consider a 20 km-grid mesh a minimum requirement to resolve such forcings adequately. Even with a 20 km grid, the smallest feature that a model adequately resolves is about 100 km in length. We are not confident to resolve the strong baroclinic forcing at major oceanic fronts with the resolution lower than T639. In fact, we failed to obtain the same qualitative results when we repeated the experiments with T159L48 that has a horizontal grid spacing of about 80km. Running a full atmospheric GCM at this high resolution for 2 months for 6 experiments requires an extremely strong computational power. We used the Earth Simulator to perform the experiments.

AFES was initialized with the analyzed fields at 00UTC July 1 2003 obtained from Japan Meteorological Agency and integrated in time for 45 days with different SST. The control run was done with the observed daily SST and sea ice. The daily SST (RTG SST analysis by NCEP/MMAB) and sea ice ((sea ice concentration analysis by MMAB) fields are originally given on a $0.5° \times 0.5°$ mesh. Necessary interpolation was done to fit the forcing fields to the model grid. By using the observed daily SST and sea ice, we are essentially forcing the model to conform to the answer to some extent. The land urface temperature in the model, however, is internally determined and is a major uncertainty factor in the control run. After we confirmed a reasonably successful simulation of the

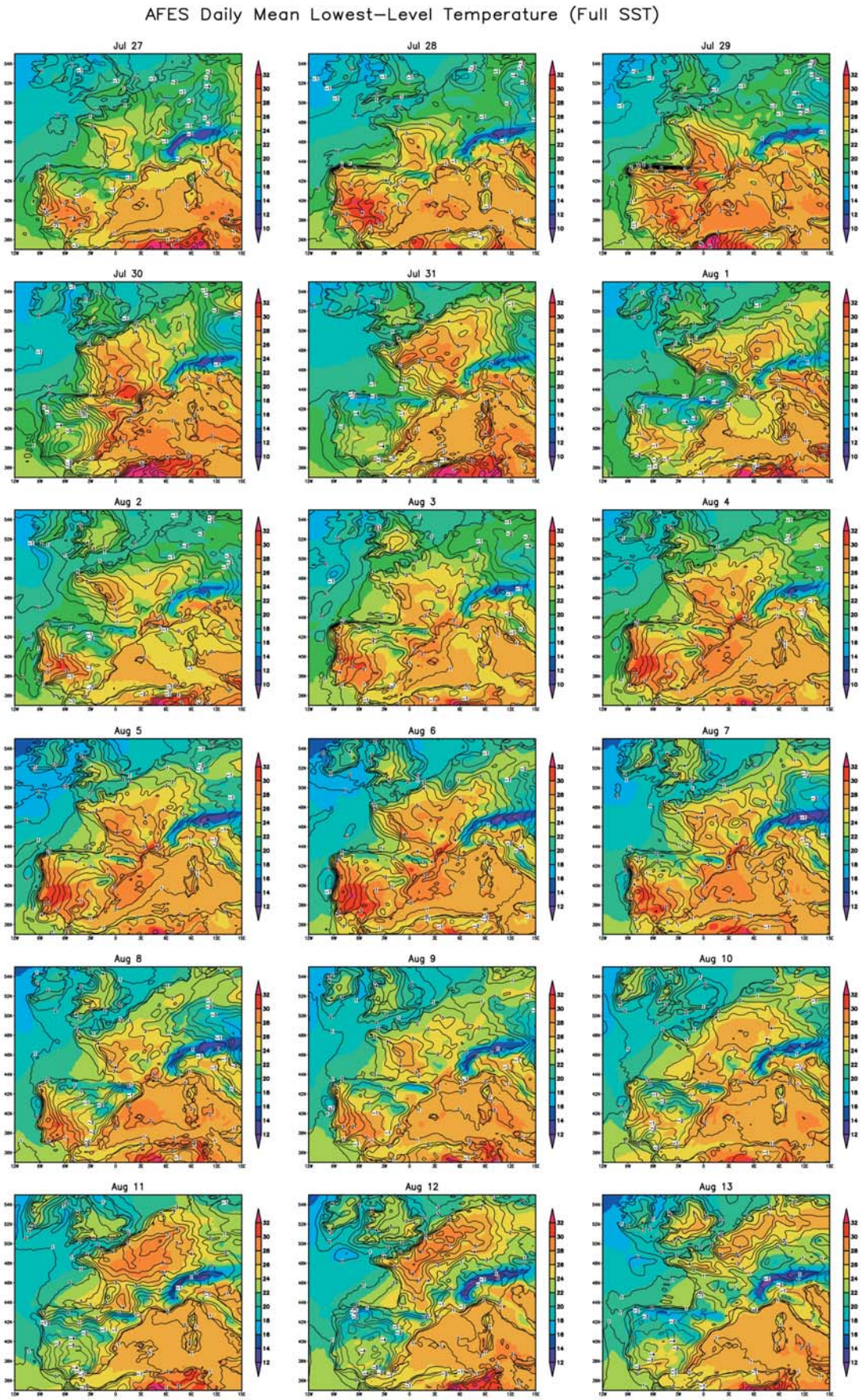

Fig. 4 The daily mean lowest-level temperautre (color shade) in the control run (run C) and its departure (contours) from the average of 5 non-heatwave runs (runs E1, E2, E3, E4, and E5), simulated by AFES.

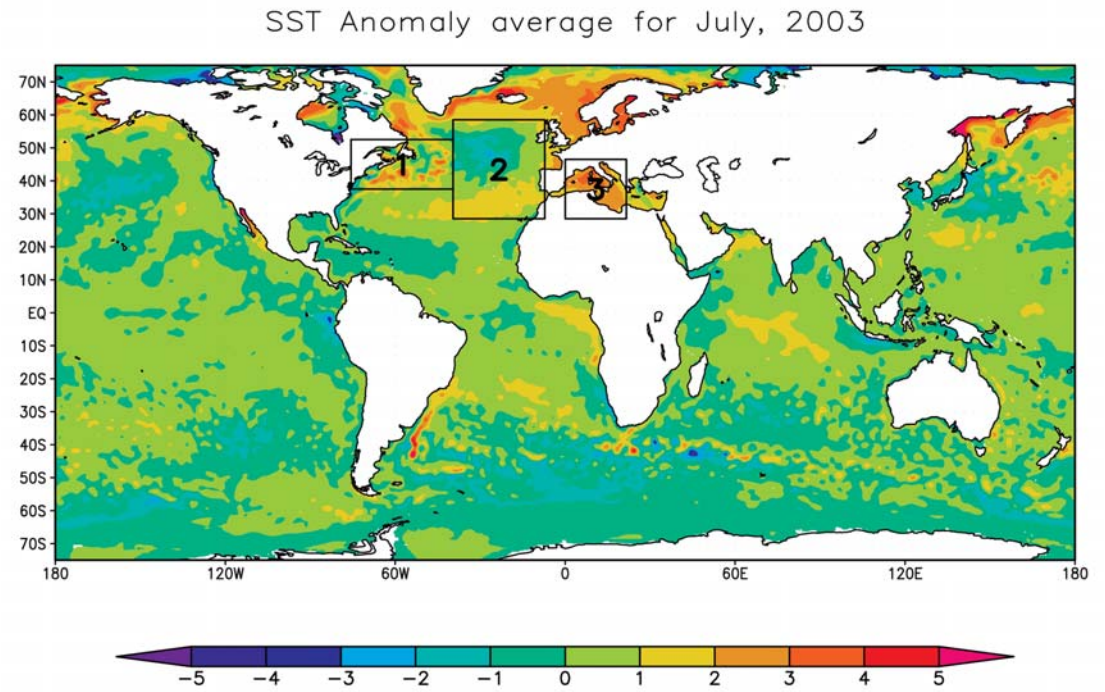

Fig. 5 The SST anomaly averaged over a month, July 2003. The daily SST, the Real Time Global SST analysis, is provided by the Marine Modeling and Analysis Branch of NCEP, while the climatological SST is from the UK Hadley Center. They were interpolated linearly in time.

heatwave in the control run, we carried out 5 experimental runs with the SST replaced with the climatology in specific region(s) or everywhere. The control run and 3 experimental runs that exhibited low-frequency evolutions that are visibly different from the control run were extended for 15 days for further diagnoses of the kind described in the previous section. In all runs, only the daily mean of key model fields were archived due to the limitations on our archival resources. Six-hour mean would have been much more desirable for our diagnoses, but would had have generated prohibitively large output.

2.2 Simulation results

The control run (run C, from here on) reproduced the heatwave reasonably well after about one month of forced integration. Figure 4 shows the daily mean temperature (color shade) of the lowest model level, roughly 50 m above the surface, and its departure from the average of 5 experimental runs that did not reproduce the full-grown heatwave to be mentioned later (contours). Note that the temperature at the lowest model level is slightly lower than the surface temperature. The simulated heatwave begins on July 27, 5 days earlier than the observed, and ends on August 13, 2 days earlier than the observed. The overall pattern and evolution of the simulated near-surface temperature compare fairly well with those of the estimated daily mean surface temperature shown in Fig 1. The intensity of the simulated heatwave appears somewhat weaker than the observed when Fig 1 and Fig 4 are compared. Still, the daily mean temerature at the model's lowest level (not the surface) is above 26°C in a large part of France, exceeding 30°C in some isolated spots, during the simulated heatwave.

Table 1 AFES runs and region(s) in which the climatological SST is used for the runs. Daily observed SST is used in the control run, C. See Fig. 4 for the location of the "Regions". The presence of the "Heatwave" was determined by visually inspecting the daily mean lowest-level temperature in late July and first 2 weeks of August in the simulation.

Run	Clim SST	Heatwave
C	None	Yes
E1	Everywhere	No
E2	Regions 2 and 3	No
E3	Region 2	Yes
E4	Region 3	Yes
E5	Region 1	No

Following a reasonably successful simulation of the heatwave in run C, we performed 5 experiments in which the SST used in run C was replaced with the climatology (monthly means interpolated to each time step) entirely or partially. Figure 5 shows the SST anomaly in the daily data with respect to the daily interpolated climatology averaged over the month of July 2003. We focused on 3 regions, enclosed in numbered rectangles, because of the

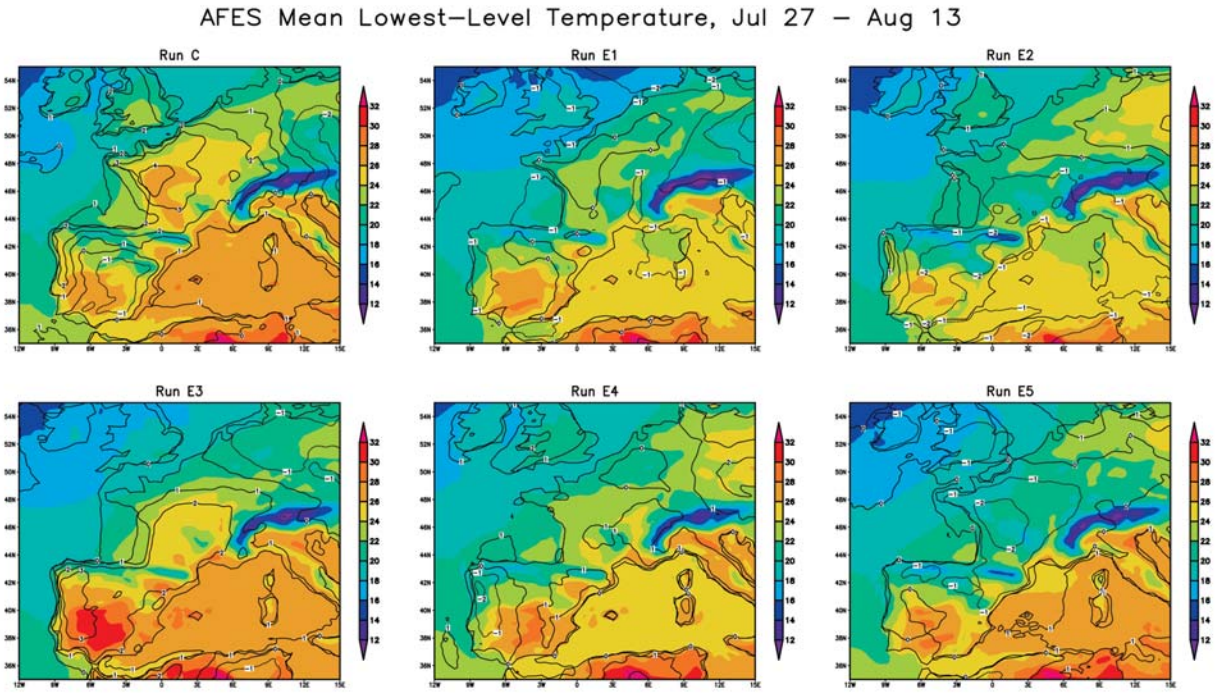

Fig. 6 The mean lowest-level temperature (color shade) and its departure (contours) from the average of E1, E2, E3, E4, and E5 for the heatwave period in run C, Jul 27 – Aug 13. Run C (upper left), run E1 (upper center), run E2 (upper right), run E3 (lower left), run E4 (lower center), and run E5 (lower right) are shown.

following reasons. The SST anomaly in Region 1, the vicinity of the Gulf Stream, has a high potential for altering the large-scale background flow in the middle-latitude North Atlantic and wave generation in and downstream of the region. The SST gradient across the Gulf Stream in reality is much larger than that given in the climatological atlas that has smoothed the actual fields into an extremely coarse grid. Of course, a model atmosphere is not capable of sensing such a large concentrated SST gradient unless the model's horizontal resolution is at least 20 km or so. The dipole-like anomaly in Region 2 tends to enhance the eastward advection of waves at upper levels and also to aid wave growth where the low-level baroclinicity is enhanced. The warm anomaly in Region 3 has a potential for altering behaviors of waves that enter the southwestern Europe through changes in the low-level baroclinicity, and may have a simple local warming effect on the areas surrounding the Mediterranean Sea.

In experiment 1 (run E1), we used the climatological SST everywhere. In experiment 2 (run E2), we used the climatology in the northeastern North Atlantic (Region 2) and the Mediterranean (Region 3). Experiment 3 (run E3) was run with the climatology in the northeastern North Atlantic only, while experiment 4 (run E4) was run with the climatology in the Mediterranean only. Finally, we used the climatology in the northwestern North Atlantic (Region 1) in experiment 5 (run E5). A list of all the simulation runs and the SST used in the runs is given in Table 1, along with a subjective judgement on the runs' success or failure in generating a heatwave. The regional replacement of observed daily SST with the climatology was done with a smooth transition along the border of the replaced regions with an e-folding scale of roughly 300 km. The choice of removing and not adding anomalies in a selected region(s) reflects our belief that a highly nonlinear phenomenon of this kind is not likely to be a product of an anomalous forcing in one region, but a product of anomalous forcings in multiple regions. If our belief is correct, then the model would not be able to produce the phenomenon even if an important anomaly is added to one region. Since we do not have the resource to perform ensemble experiments at this resolution, we choose to remove potentially important anomalies from the daily SST. The initial condition and other forcings are the same as those used in run C.

The simulated atmospheres in all 5 experiments are essentially the same as that in run C during the first few days of the simulation. Since the initial condition, including the low-frequency planetary-scale features, contains effects of the actual forcing up to July 1 2003, the first week or two of these experiments should be considered as an adjustment period. To summarize the results of the 5 experiments, all but run E3 failed to produce a heatwave. Run E4 produced some signs of a heatwave, but visibly weaker than those in run E3, not to mention run C. For a quick comparison, the average lowest-level temperature

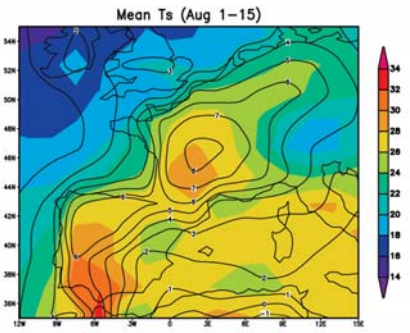

Fig. 7 The mean surface temperature for Aug 1 – 15, 2003, estimated from NCEP/NCAR 6-hourly reanalyses.

(color shade) and its departure from the average of the 5 experimental runs during July 27 – August 13 in run C and the 5 experiments are shown in Fig 6. The estimated average surface temperature (color shade) and its departure from the 30-year climatology (contours) for the actual heatwave for August 1 – 15 are shown in Fig 7. Again, note that the lowest-level temperature in the model should be somewhat lower than the surface temperature. Runs E1, E2, and E5 clearly failed to produce a heatwave, while run C compares reasonably well with the actual event. The departure of the daily mean lowest-level temperature in run C from the average of the 5 experimental runs during the simulated heatwave period is typically 3°C and larger, reaching 8°C in some spots (Fig. 4).

2.3 Diagnoses of simulations

After these 45-day integrations, we extended run C and run E1, E2, and E5 for 15 days to compute low-frequency quasi-geostrophic potential vorticity (QGPV) and high-frequency quasi-geostrophic transient wave activity fluxes defined by Plumb [7]. The purpose of these calculations is to examine if the simulated heatwave was caused by an eastward-shifted blocking as in the observed case, and also to compare the high-frequency transient wave forcing in these simulations to the observed with a hope of identifying the cause of the eastward shift in the blocking location.

Figure 8 shows, for run C and run E1, E2, and E5, low-freuency QGPV at 200hPa every 3 days from July 27, the beginning day of the simulated heatwave in run C. The model output on sigma levels was linearly interpolated to compute these quantities. A simple low-pass filter [8] with a 10-day cut-off is used here. Due to the extremely high resolution of the model output, for plotting purposes only, the horizontal resolution is reduced to roughly $2° \times 2°$ by area-weighted averaging. The simulated blocking in run C is very strong, but somewhat displaced westward of the observed. Nevertheless, western Europe is within the area of influence of the blocking ridge (note that the peak of the blocking ridge penetrates into 60°N, 0°E during the peak stage), resulting in higher low-level temperatures compared to other experiments. In each of runs E1, E2, and E5, a strong blocking does occur, but visibly shifted westward compared to run C. Western Europe is outside the area of influence of the blocking ridge in these 3 experiments. Instead, to varying extents, western Europe is under the influence of a low-frequency trough just downstream of the blocking ridge. This difference in the location of the blocking is reflected clearly in the mean near-surface temperature during this period shown in Fig 6.

Nakamura et al. [5] demonstrated for winter blocking events in the North Atlantic and North Pacific that evolution of a blocking is primarily controlled by low-frequency advection. They further demonstrated that contribution of synoptic-scale high-frequency waves to low-frequency flow forcing is not negligible, although not dominant either, and depends on the location of blocking occurrence. Although the degree to which synoptic-scale high-frequency waves contribute to a blocking varies, probably from an event to another event, convergence of transient wave activity into the region of blocking during the formation stage has been clearly shown [5, 9]. It is consistent with other observational studies [10] and idealized model experiments [11]. The pioneering work by Shutts [11] clearly demonstrated that the relative strength of a localized wave forcing with respect to the background flow advection is the key factor in generating a blocking. This condition can be created by zonally inhomogeneous or locally enhanced low-level baroclinicity alone. In the presence of topography, the "localized wave forcing" can be generated by the organizing effect of the topography-forced background flow on synoptic-scale high-frequency waves. Regardless of the configuration in which the localized wave forcing is arranged, wave forcing upstream of the blocking region and convergence of the wave activity in the blocking region are essential ingredients of the blocking dynamics. We focus on this aspect of the blocking dynamics here.

One key factor necessary for blocking generation is the propensity of the large-scale environment to accumulate wave activity locally. This condition may be provided in several different ways. An easy configuration that provides such a condition is a region of weak baroclinicity paired with a region of strong baroclinicity upstream - wave activity tends to accumulate in the region of weak baroclinicity due to the weaker zonal advection by the upper tropospheric flow and its deformation field [4]. One plausible reason for an eastward shift of blocking in our case, summer blocking over Europe, is that the low-level baroclinicity over the eastern North Atlantic, where baroclinicity is weak, was stronger than usual. Another plausible reason is an eastward extension (from its usual

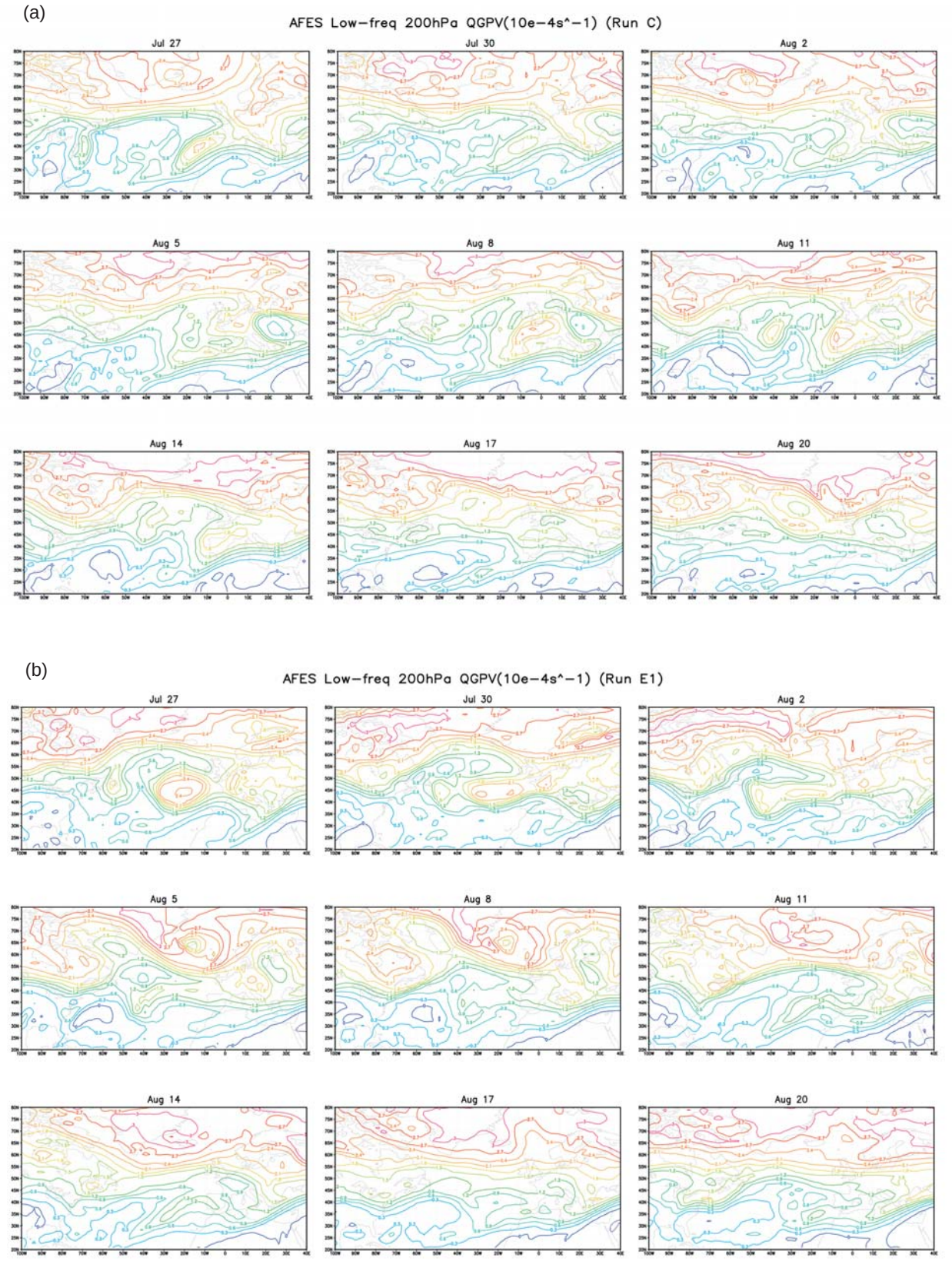

Fig. 8 Low-frequency quasi-geostrophic potential vorticity ($10^{-4}s^{-1}$) at 200hPa shown every 3 days from Jul 27 to Aug 20 2003, calculated from AFES output of (a) run C, (b) run E1, (c) run E2, and (d) run E5. The low-frequency cut-off used in the filter is 1/10days.

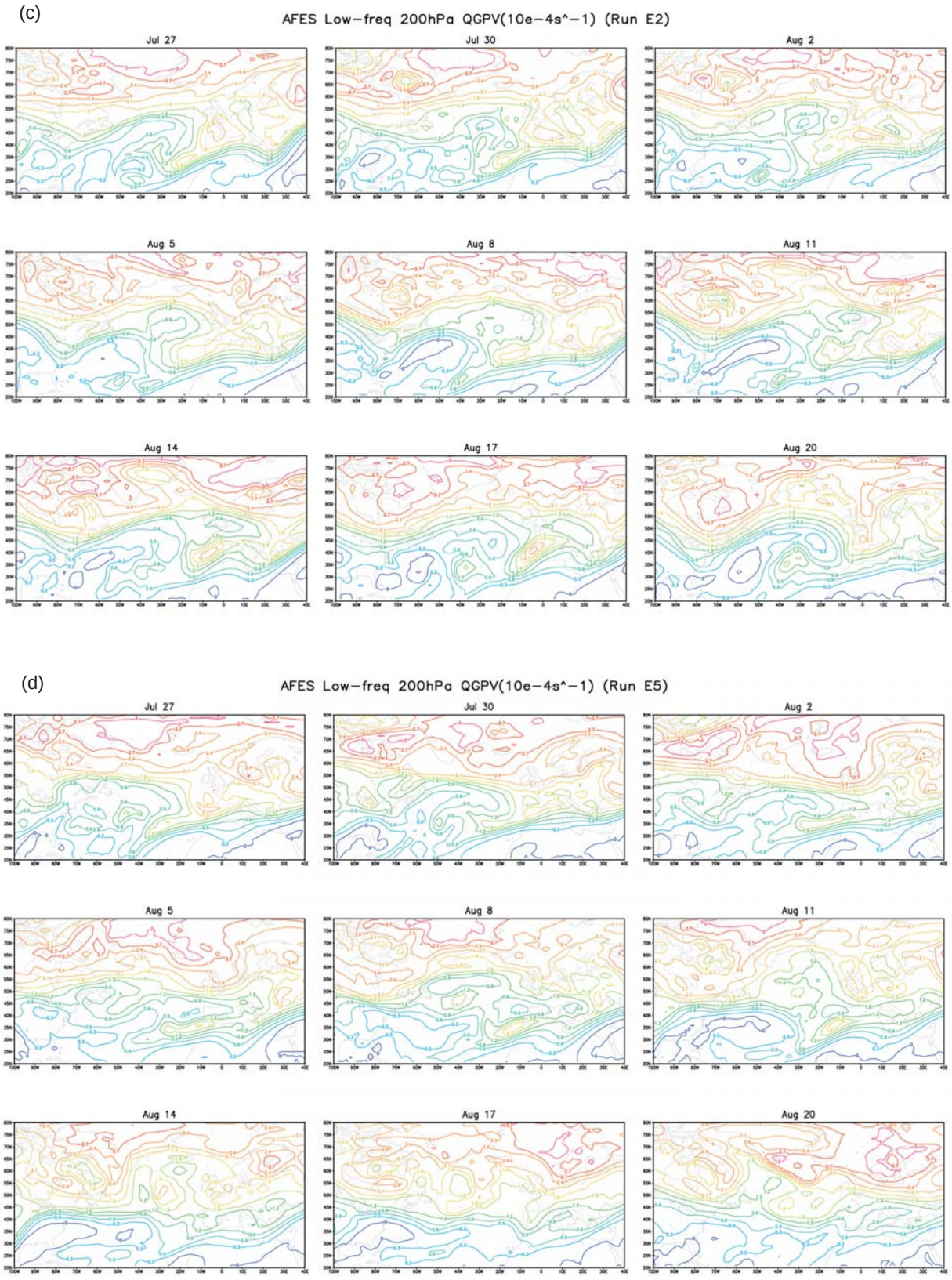

Fig. 8 (continued).

range) of high baroclinicity region in the western North Atlantic. Enhanced wave generation over the western North Atlantic and/or North Pacific can induce a blocking in the eastern North Atlantic, and can elevate the intensity of blocking, but tends to shift the blocking westward, not eastward, through the eddy feedback discussed in many previous studies [12].

A useful diagnostic tool to study transient wave generation, propagation, and dissipation is the three-dimensional quasi-geostrophic transient wave activity and its fluxes defined by Plumb [7]. Quasi-geostrophic transient wave activity, M, is defined by $M = \frac{\overline{q'^2}}{|\nabla_h \bar{q}|}$, where $\bar{q}$ and q' are, respectively, the mean and perturbation quasi-geostrophic potential vorticity. By dividing the variance of q by the magnitude of the horizontal $\bar{q}$ gradient, we obtain a measure of transient quasi-geostrophic wave amplitude. Plumb [7] derived a set of equations for M fluxes that describes the three-dimensional propagation of linear quasi-geostrophic transient waves in a slowly-varying (with respect to the spatial structure of the transience) mean state. The equations connect the divergence and convergence of the fluxes to the source and sink of wave activity, respectively. We use Plumb's formula with a time-varying field separation into low-frequency and high-frequency, rather than the time mean and deviation from the mean. In other words, at each time frame available, low-frequency evolution of high-frequency wave action on the low-frequency field at the same time frame is calculated. By doing so, we can examine evolutions of M fluxes along with those of, for example, low-frequency QGPV for details when necessary. Since we identify blocking events as discretized low-frequency phenomena that are evolving, the separation of time-dependent fields into low-frequency and hih-frequency is more suitable for our study. The low-frequency filter used for these calculations is the same as that mentioned earlier [8].

Figure 9 shows the vertical flux at 500hPa (upper panel) and horizontal flux and its time-integrated divergence at 200hPa (lower panel) of high-frequency wave activity averaged over 12 days that precede the blocking in run C, Jul 15 – 26. The fields shown in Fig 9 are noisier than those calculated from the reanalyses data due partly to the high-resolution of the model, but also to the coarse output archiing frequency - daily averages. We performed the calculations with the original daily mean output and with an artificially expanded output, a 5-times-per-day output that was created by linearly interpolating the original daily output in time. We found only minor differences in the noisiness of the results obtained from the 2 sets of calculations, while the qualitative aspect of the results was the same. Somewhat less noisy results obtained from the calculations with the artificially expanded output are used in the figures.

The 500hPa vertical flux field in run C (Fig 9a) shows some qualitative resemblance to the observed (not shown), although the magnitude is somewhat smaller. The fact that the original model output is given as daily averages is partly responsible for the relative smallness of the maginitude. Two regions of strong upward flux seen in the reanalyses data, one in the central North Pacific and the other in the vicinity of the Great Lakes in North America have been reproduced, while another region of strong upward flux in the northern fringe of Canada is only vaguely reproduced. A region of large vertical flux in the central North Atlantic, suspected as a potential cause of the eastward shift of the blocking, also shows some upward flux in run C, although significantly smaller than the observed. The horizontal flux at 200hPa also shows some qualitative resemblance to the observed (not shown). The divergence field is much noisier than the observed. However, perhaps the key feature of the field, the large divergence above the region of upward flux in the central North Atlantic and the meridionally elongated areas of convergence immediately downstream, is present in run C also.

We now examine the wave activity flux fields in runs E1, E2, and E5 (Fig 9b, 9c, and 9d) and compare with those in run C. In run E1, forced with the climatological SST everywhere, both the vertical and horizontal flux fields are completely different from those in run C. The region of upward flux in the central North Atlantic is absent in run E1. So is the pair of horizontal flux diverege-nce and convergence. In this run, a region of strong upward flux is located over North America to the north of the Greak Lakes. Also, the pair of horizontal flux divergence and elongated band of convergence immediately downstream is located near the western boundary of the North Atlantic with its divergence part coinciding with the region of upward flux down below. These features imply that high-frequency wave forcing was in favor of creating the blocking just off the east coast of North America, not near western Europe. The wave activity flux structures in run E2 are, again, quite different from those in run C and run E1. However, a tendency for high-frequency wave forcing from down below to trigger a blocking growth close to the east coast of North America, similar to that in run E1, can be seen. There are some spots of upward flux in the central North Atlantic. But they are not very strong and not accompanied by substantial horizontal flux divergence above. Finally, in run E5, the 500hPa vertical flux field roughly resembles that in run C. There is a meridionally elongated region of upward flux in the central North Atlantic that appears, by itself, as if it tends to help gener-

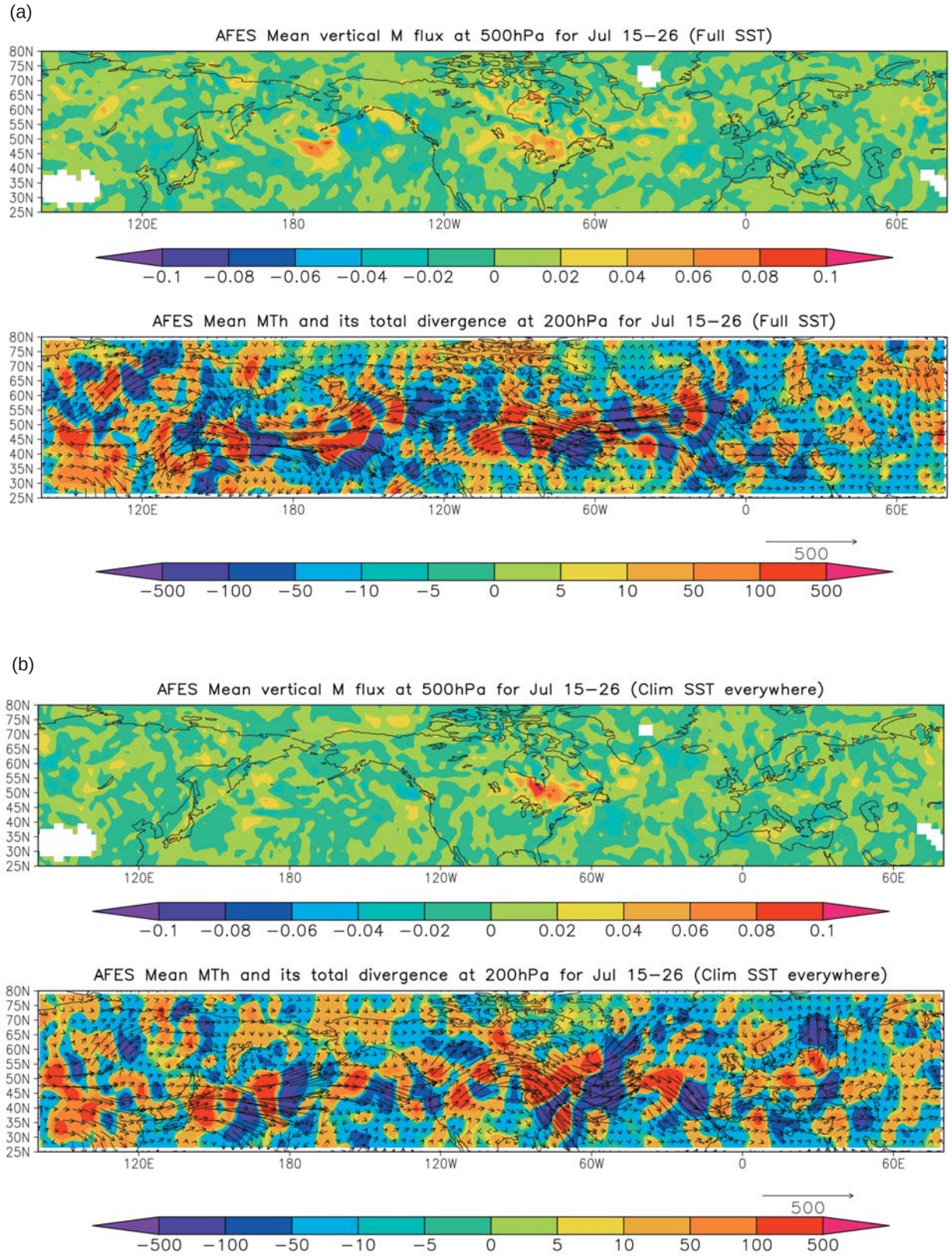

Fig. 9 The vertical flux at 500hPa (upper panels) and the horizontal flux at 200hPa (arrows in lower panels) of the high-frequency quasi-geostrophic transient wave activity flux (m^2s^{-2}) averaged over 12 days, Jul 15-26, the period preceding the heatwave in run C. The lower panels also shows the time-integrated divergence of the hirizontal flux (ms^{-1}) during the period. Shown are (a) run C, (b) run E1, (c) run E2, and (d) run E5.

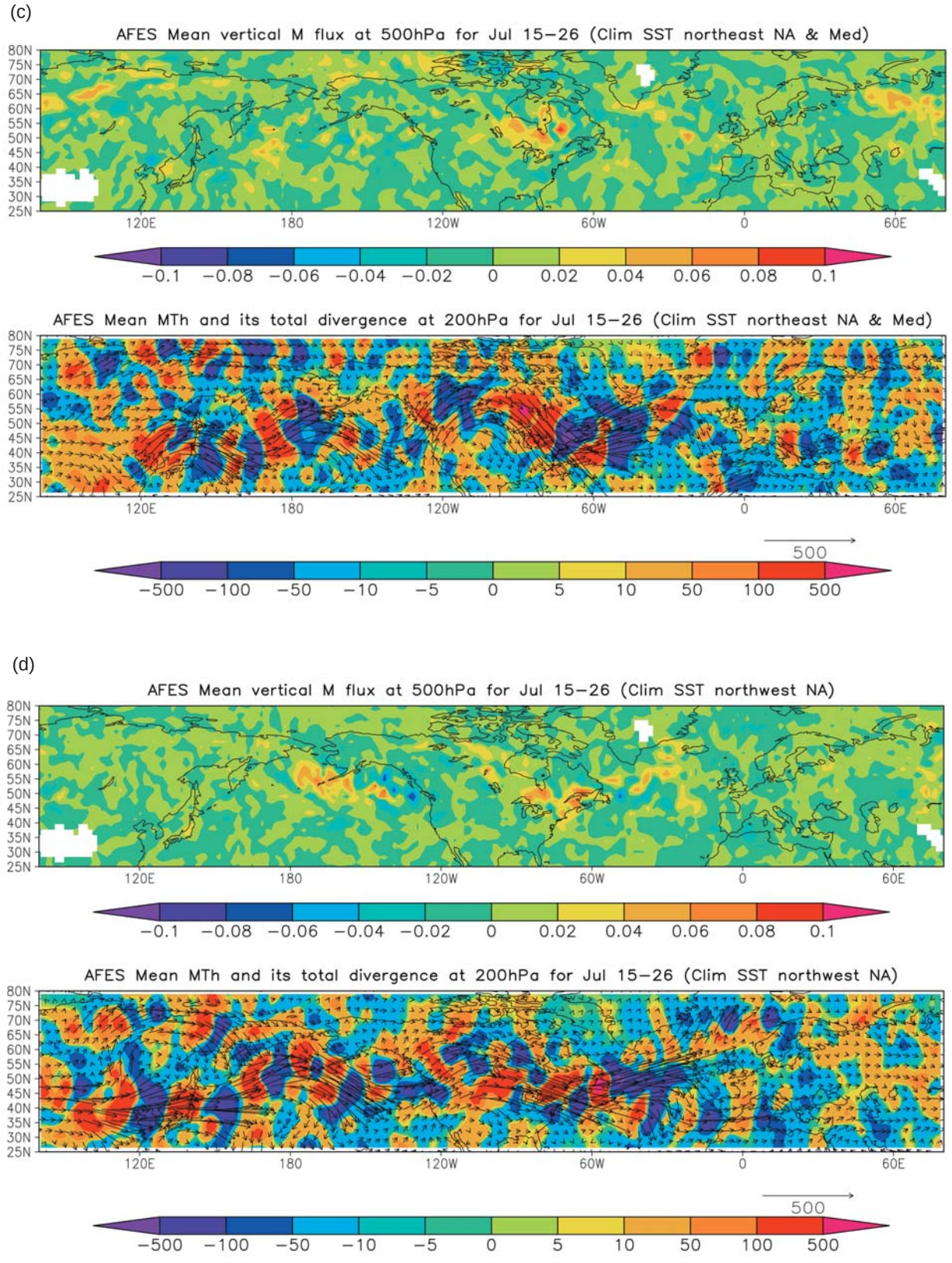

Fig. 9 (continued).

ate a blocking closer to western Europe. However, the horizontal flux and its divergence fields at 200hPa suggest that the upward fluxes in the region, after reaching upper levels, are diverted north and south away from the region of blocking growth, hence, not contributing to the blocking. In fact, there is a large region of strong horizontal flux convergence in the western to central North Atlantic, centered at around 40°W and 50°N, just downstream of a region of strong upward flux over the northeastern U.S./eastern Canada, that tends to aid the growth of a blocking in the central North Atlantic.

The relationship between the SST anomaly removal in run E1, E2, and E5 and wave forcing differences found in the simulation runs is not simple and cannot be determined unambiguously. We can only speculate on it here. First, in run E1, we expect the wave forcing to be completely different from that in run C, since the climatological SST was used everywhere in run E1. If we are to focus on the combined effect of removing the SST anamolies in regions 1, 2, and 3, then it would be to reduce wave generation and advection over the North Atlantic, because of the reduced baroclinicity in both regions 1 and 2. Strong baroclinicity in the northern hemisphere during July is found over middle North America to the east of the Rockies. Reduced baroclinicity in regions 1 and 2, therefore, tends to generate a blocking over the western North Atlantic by aiding accumulation of wave activity there. This difference is indeed found between run C and run E1 (compare Figs 9a and 9b).

In run E2, eastward wave activity advection is reduced over the eastern North Atlantic by the removal of the SST anomaly in region 2. At the same time, the removal of the SST anomaly in region 3 tends to reduce the eastward wave advection and generation in southern Europe by reducing the low-level baroclinicity, and also has a local cooling effect. Since strong wave activity generation over North America and the western North Atlantic is intact, the removal of the SST anomalies in regions 2 and 3 tends shift the location of wave activity accumulation westward to the central North Atlantic. Careful comparison of Figs 9a and 9c shows that it is indeed the case - substantially less wave activity reaches the eastern North Atlantic and western Europe in run E2 than in run C.

Finally, in run E5, the reduced low-level baroclinicity in region 1 should result in reduced eastward wave activity advection and wave generation over the western North Atlantic. This, of course, leaves the enhanced eastward wave advection in region 2 intact, but substantially reduces the wave advection into region 2 at the same time. Consequently, we expect the reduced baroclinicity in region 1 to aid accumulation of wave activity in the western North Atlantic, thereby shifting the blocking westward in run E5. This expectation, however, is not met exactly. When one compares Figs 9a and 9d, one finds that the wave activity reaching western Europe is significantly less in run E5 than in run C. Also, large horizontal flux convergence in run E5 is located over the central North Atlantic, while that in run C is located near the eastern fringe of the North Atlantic and western Europe. These two features are in accord with our expectation. However, when the differences in the wave forcing fields between run C and run E5 are plotted (not shown), we find the horizontal wave activity flux in region 1 larger and eastward than in run C. There is no clear sign of this extra flux arriving from upstream, suggesting that the difference is mostly locally generated. This is clearly contrary to our expectations. We do not have a good explanation for this unexpected response of the model atmosphere.

In short, the high-frequency wave forcing in runs E1, E2, and E5 tends to shift the blocking westward compared to run C. Thus, the series of experiments presented here suggest that the high-frequency wave forcing was a key factor in the eastward shift of the blocking that resulted in the heatwave of August 2003 in western Europe. They further suggest that providing an accurate high-resolution SST field to an atmospheric model is necessary to simulate the low-frequency behavior of the atmosphere, especially when the behavior is highly nonlinear. The response of the model atmosphere is, as demonstrated here, very sensitive to the SST field in the vicinity of the Gulf Stream where the SST gradient is much larger than a typical value.

3. Concluding remarks

We presented here diagnoses of the heatwave that hit western Europe during the first half of August 2003, using the NCEP/NCAR reanalyses and simulation output of AFES. Based on the diagnostic results, we suggest that a key factor that made the blocking event of August 2003 occur over Europe, not over the North Atlantic, was an eastward extension of the band of moderately strong baroclinicity along the North Atlantic storm track. We emphasize that the blocking generation *per se* did not depend on the eastward extension of the North Atlantic baroclinic zone. If indeed the eastward shift in the blocking location that made the event a catastrophe was caused by the persistent high-frequency wave forcing coming from below, a coarse-resolution model (perhaps even T639 used here) is unlikely to simulate the event well even if all the external forcings, including the SST, are given. This is because the model cannot adequately resolve the nonlinear processes involved in the positive feedback of high-frequency waves onto the diffluent low-frequency flow, i.e., breaking of the high-frequency waves, generation of filaments and detached small vortices, and "deposition" of the potential

vorticity associated with the filaments and vortices in the low-frequency field. What happens in this "deposition" process in reality is a decrease in the evolution rate of these synoptic-scale waves and filaments and vortices that are generated by the breaking of the waves as they enter the region of the blocking. The vortices and filaments evolve slowly within the region, but do not disappear immediately. When they do lose their physical identities, their potential vorticity is not lost diffusively, but is mixed with the surrounding circulations. In other words, this mixing process is not necessarily down the gradient of the low-frequency field. Coarse-resolution models that cannot adequately resolve these filaments and vortices of order tens to hundreds of kilometers are too diffusive to accurately simulate a highly nonlinear phenomenon of this kind.

On the other hand, based on our modest success in hindcasting the blocking of August 2003 roughly a month in advance, we suspect that forecasting phenomena whose dynamics are essentially low-frequency a few to several weeks in advance may become possible in the future. Of course, such forecasting skills depend on the model's ability to forecast the SST and land surface temperatures, in addition to its ability to accurately represent the internal dynamics of the atmospheric low-frequency state. This means that such a long-range forecast model must have the atmosphere up to the top of the stratosphere, all oceans, the land surface, and perhaps the ice, interacting dynamically and thermodynamically with each other. Needless to say, the model must be able to accurately represent those second-order variables, such as the cloudiness, precipitation, and soil moisture, that are important for low-frequency forcing. Finally, but never the least, observational network must be improved to provide a reasonable initial condition to the forecast model. In the light of long evolution time scales of planetary-scale waves, having an accurate initial condition that extends up to the upper stratosphere is critical to a reasonably accurate simulation of the low-frequency evolution of the atmosphere. The next generation of super computers will be probably large and fast enough to handle the task. We must stride to prepare the soft tools and the input data for the task. When all the necessary ingredients become available, we shall see how far ahead we can predict the low-frequency atmospheric state.

Acknowledgment

Model integration and output diagnoses were done on the Earth Simulator maintained by the Earth Simulator Center. We are grateful to Dr. Ohfuchi and Mr. Yamada for various support and assistence in running experiments with AFES. We also wish to thank Dr. Slingo for comments that were helpful in improving the manuscript.

(This article is reviewed by Dr. Julia Slingo.)

References

[1] E. Kalnay, M. Kanamitsu, R. Kistler, W. Collins, D. Deaven, L. Gandin, M. Iredell, S. Saha, G. White, J. Woollen, Y. Zhu, M. Chelliah, W. Ebisuzaki, W. Higgins, J. Janowiak, K. C. Mo, C. Ropelewske, J. Wang, A. Leetmaa, R. Reynolds, R. Jenne, and D. Joseph, The NCEP/NCAR 40-year Reanalysis Project, *Bull. Amer. Meteor. Soc*., vol.**77**, pp.437–471, 1996.

[2] E. Black, M. Blackburn, G. Harrison, B. Hoskins, and J. Methven, Factors contributing to the summer 2003 European heatwave. *Weather*, vol.**59**, pp.217–223, 2004.

[3] C. Schär, P. L. Vidale, D. Lüthi, C. Frei, C. Häberli, M. A. Liniger, and C. Appenzeller, The role of increasing temperature variability in European heatwaves. *Nature*, vol.**427**, pp.332–336, 2004.

[4] M. Nakamura, Characteristics of potential vorticity mixing by breaking Rossby waves in the vicinity of a jet. *Sc.D. thesis*, Massachusetts Institute of Technology, Cambridge, Massachusetts, U.S.A., 1994.

[5] H. Nakamura, M. Nakamura, and J. L. Anderson, The role of high- and low-frequency dynamics in blocking formation. *Mon. Wea. Rev*., vol.**125**, pp.2074–2093, 1997.

[6] W. Ohfuchi, H. Nakamura, M. K. Yoshioka, T. Enomoto, K. Takaya, X. Peng, S. Yamane, T. Nishimura, Y. Kurihara, and K. Ninomiya, 10-km mesh meso-scale resolving simulations of the global atmosphere on the Earth Simulator – Preliminary outcomes of AFES (AGCM for the Earth Simulator). *J. Earth Simulator*, vol.**1**, pp.8–34, 2004.

[7] R. A. Plumb, Three-dimensional propagation of transient quasi-geostrophic eddies and its relationship with eddy forcing of the time-mean flow. *J. Atmos. Sci*., vol.**43**, pp.1657–1678, 1986.

[8] N. C. Lau, and K. M. Lau, The structure and energetics of midlatitude disturbances accompanying cold air outbreaks over East Asia. *Mon. Wea. Rev.*, vol.**112**, pp.1309–1327, 1984.

[9] H. Nakamura, Rotational evolution of potential vorticity associated with a strong blocking flow configuration over Europe. *Geophys. Res. Let*., vol.**21**, pp.2003–2006, 1994.

[10] G. J. Shutts, A case study of eddy forcing during an Atlantic blocking episode. *Advances in Geophysics*, vol.**29**, Academic Press, pp.135–161, 1986.

[11] G. J. Shutts, The propagation of eddies in diffluent jetstreams: Eddy vorticity forcing of 'blocking' flow fields. *Quart. J. Roy. Meteor*., vol.**109**, pp.737–761, 1983.

[12] K. Haines, and J. C. Marshall, Eddy-forced coherent structures as a prototype of atmospheric blocking. *Quart. J. Roy. Meteor*., vol.**113**, pp.681–704, 1987.